Noname manuscript No.
(will be inserted by the editor)

Landmark assisted Location and Tracking in Outdoor Mobile Network

Marco Anisetti, Claudio A. Ardagna,
Valerio Bellandi, Ernesto Damiani,
{*firstname.lastname*}@unimi.it,
Mario Döller, Florian Stegmaier,
Tilmann Rabl, Harald Kosch,
{*firstname.lastname*}@uni-passau.de and
Lionel Brunie,
lionel.brunie@insa-lyon.fr

Abstract Technical enhancements of mobile technologies and the integration of multi-sensors, like accelerometer and camera, within mobile devices are paving the way to the definition of high quality and accurate geolocation solutions based on the informations acquired by multimodal sensors, and data collected and managed by GSM/3G networks. In this paper, we present a technique that provides geolocation and mobility prediction of a mobile devices, mixing the location information acquired with the GSM/3G infrastructure and a landmark matching obtainable thanks to the camera integrated on the mobile devices. We first present our geolocation approach based on an advanced Time-Forwarding algorithm and on database correlation technique over Received Signal Strength Indication (RSSI) data. Then, we integrate it with a landmark recognition infrastructure, to enhance our algorithm in those areas with poor signal and low accurate geolocation. The radio signal-based location is thus improved integrating the information gettable via landmark recognition infrastructure directly in the geolocation algorithm. Finally, the performances of the geolocation algorithm are carefully validated by an extensive experimentation, carried out on real data collected from the mobile network antennas of a complex urban environment.

Keywords Landmark · Geolocation · Wireless network

1 Introduction

Wireless and mobile technologies have radically changed the way in which users communicate, interact, and stay online. The accuracy and reliability of such technologies, and the availability of low cost handheld devices enable users to communicate and interact anywhere anytime. As a consequence, information on the location and mobility

Marco Anisetti, Claudio A. Ardagna, Valerio Bellandi, and Ernesto Damiani are with Università degli Studi di Milano (Italy). Mario Döller, Florian Stegmaier, Tilmann Rabl, and Harald Kosch with the University of Passau (Germany). Lionel Brunie with the INSA Lyon (France).

of the users are easily available and just becomes one class of personal information associated with their identity. This ubiquitous scenario fostered the development of new and online applications that need location information of the users to offer their services. Location-Based Services (LBSs), such as, navigation, instant messaging, friend finder, and points of interest, have received great attention in the near past and gained popularity. Although some of the above services only require a rough localization of the mobile terminal, others have also been deployed for scenarios (e.g., emergency rescue) where the geolocation precision plays a fundamental role.

Many geolocation algorithms are currently available and exploit different peculiarities of the cellular network. For instance, many algorithms are based on time measurements (e.g., [14, 21]), while others are based on signal strength and electro-magnetic field prediction (e.g., [1, 13, 27]). An important aspect of the geolocation problem is that it is usually difficult to provide a general solution that works well regardless of the considered environment (e.g., urban, suburban, rural). In addition, cellular geolocation in urban environments is a difficult task since physical phenomena, such as, signal reflection, diffraction, penetration, scattering, fluctuation, can influence the quality of geolocation. In this scenario, the consideration of timing and strength of the signal as the only information available for the mobile geolocation is limiting. Mobile devices in fact are more than simple mobile phones that join the cellular network; rather they are multi-sensor devices that include accelerometers, high-quality digital camera, WiFi cards, GPS receivers. Recently, some solutions have used additional information coming from these sensors to improve geolocation or LBS functionalities. As an example, in the recent 3G version of the iPhone a GPS chipset was added; the AGPS (Assisted GPS) [9] has been designed to use WiFi Positioning System (WPS) together with cell data to speed up the acquisition of the GPS signal. The iPhone on-board accelerometers are also used to improve GPS-based location accuracy at low speeds (walking or biking). In addition, mTourist [11] is a LBS that uses geolocation and landmarks to guide the tourists through a city. Using the integrated camera, the devices take some pictures of sorrouding buildings, which are then matched with a database of buildings to identify the current position of the users.

Next generation geolocation algorithms and LBSs can take advantages by enhancements in mobile devices and by the availability of new information, so to provide high quality and accurate services. In this paper, we study the effects of the integration of a high-accurate geolocation technique based on signal strength with a landmark recognition infrastructure. In particular, we present how a smart integration can provide benefits for the location techniques providing accurate geolocation also in those areas that are not covered by a reliable signal. We take as a reference our geolocation solution based on Received Signal Strength Indication (RSSI) [1] and on data normally collected and managed by GSM/3G networks, and the landmark infrastructure presented in [11]. Our landmark-based geolocation solution allows high-accurate geolocation and mobility prediction also in critical areas, by considering the exact locations retrieved by means of landmark matching.

The contribution of the paper is as follows. First, we present how the integration of a landmark recognition infrastructure that supports identification of buildings can improve our geolocation algorithm based on RSSI and DCM. The geolocation and tracking technique is improved by supplying it with those positions recognized by means of a landmark-based identification of the surrounding buildings. In other words, as soon as the landmark infrastructure system identifies a building using an image taken by the integrated camera on the device, such a position identifies a possible

location of the user that can be used to correct the geolocation algorithm. Second, we provide an extensive experimentation and a comparison between our solution in [1] and the landmark-based solution in this paper, showing performance improvements.

The remainder of this paper is organized as follows. Section 2 summarizes our past geolocation proposal. Section 3 presents the landmark recognition infrastructure. Section 4 describes our landmark-based geolocation algorithm. Section 5 shows our experimental results. Section 6 presents related work. Finally, Section 7 discusses our future work and gives our concluding remarks.

2 A Map-Based Geolocation Algorithm

Geolocation of mobile devices have been studied in several works in the area of mobile computing and resulted in several different techniques based on CellID, time measurements [14, 21], and signal strength [13, 27]. In this section, we present our geolocation strategy [1] that is used as a starting point in this paper.

2.1 DCM with Multiple Candidates

The core of the geolocation and tracking strategy is based on RSSI and Database Correlation Method (DCM) [1]. The position of a mobile terminal is determined by comparing the measurements performed by the mobile terminal itself (assuming it knows the signal strengths of the six bestserving antennas) with all entries in a lookup table [16].[1] The lookup table is a matrix that contains the predicted path loss for a given area of interest; every row in the matrix represents a single point (x,y), while each column represents a base station within the coverage area. The path loss predictions from r base stations to each given point are stored as entries in the matrix. In [1], we used a sum of squared errors between the measured path loss M_j on terminal and the path loss $E_{i,j}$ defined by entry i in the lookup table, for each antenna j. Formally, the error is calculated as $\sum_{j=1}^{r} \left(M_j - E_{i,j}\right)^2$. The point ($x$,$y$) of the entry i in the table that produces the smallest error is taken as the location of the mobile terminal.

An important aspect to consider for the accuracy of approaches based on lookup table is the quality of the Electro-Magnetic Field (EMF) prediction, which is also the largest source of error for geolocation techniques relying on DCM over RSSI. EMF prediction in fact is affected by many physical phenomena, such as reflection, diffraction, penetration, and scattering. To reduce the amount of error, many prediction models have been provided including deterministic (ray-tracing, IRT [28]), empirical (Hata-Okumura [22], Walfisch-Ikegami [8]), and hybrid (Dominant Path [29]) techniques. In [1], we provided an enhanced version of the statistic prediction model *COST231 Wallfisch-Ikegami* [8] that uses GIS information (i.e., buildings' shapes) and real antenna's shapes to make it suitable for real environments. In general, enhancing COST231 model with antennas' shapes reduces the loss in the prediction quality introduced by omnidirectional antennas, thus providing better EMF prediction quality; however, an important physical phenomenon, i.e., fluctuation, still influences the EMF prediction. Figure 1 provides a comparison between the real RSSI of a terminal (red line) and the predicted one using antenna's shapes and COST231 (black dashed

[1] This comparison can be done with many different criteria [34].

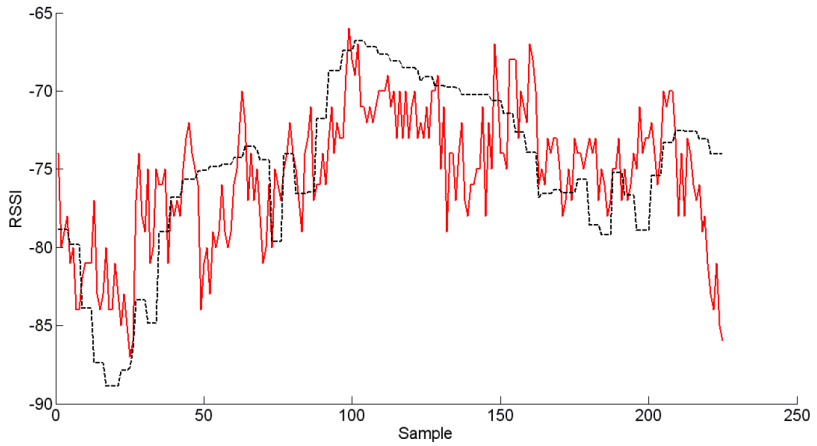

Fig. 1 Comparison between real RSSI (red line) and the estimated one (black dashed line).

line). Clearly, a solution that uses the prediction in Figure 1 is likely to provide unreliable measurements due to continuous signal fluctuations. This problem is particularly relevant in single point location techniques, as the one described above, where the difference between predicted and real EMF makes almost impossible to calculate the correct location. Often, in fact, the set of possible candidates may reside in different geographical areas and can be selected as positions in consecutive time instants resulting in low accurate geolocation.

To reduce the impact of EMF fluctuations, our approach produces a variable number n of position estimates (multiple candidates), depending on a sensibility map analysis [3]. Multiple candidates provide a considerable improvement in terms of quality, and make the solution more robust against fluctuations. As expected, the higher the number of candidates, the higher the probability of obtaining a location that better approximates the real position, at a price of an increased complexity in the candidate selection process.

2.2 Candidates selection using a time-forwarding algorithm

The next step is the evaluation of the multiple candidates to select the best one at each time instant. Our tracking method is based on a *time-forwarding algorithm* and builds on a direct acyclic graph, called *Time-Forwarding Graph* (TFG), to identify a set of paths that address GIS map and motion constraints. The time-forwarding algorithm considers a window of m time positions and for each of them n candidates. Every node in the TFG represents one of the possible positions of the mobile terminal, while edges, defined by the node pairs they connect (i.e., by source and destination nodes), represent motion between them. Each edge is associated with a weight, computed based on destination reachability and map constraints. The weight function W is defined over each edge $e = (p_{i,t}, p_{j,t+k})$, where $i, j \in [1, \ldots, n]$, $k \in [1, \ldots, m]$, and t is the actual time, as follows:

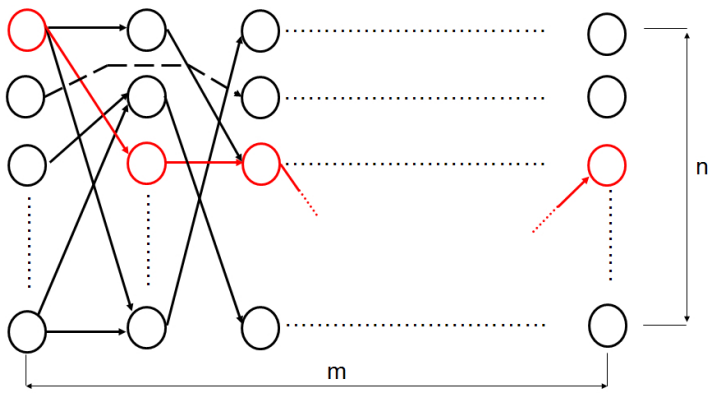

Fig. 2 TFG architecture.

$$W(e, map) = \begin{cases} \mu(e, map) & if\ \mu(e, map) \leq Th(\Delta) \\ +\infty & otherwise \end{cases} \tag{1}$$

Δ represents the time difference described by the edge e. As a result, each edge e is reachable and associated with a weight, if and only if the function μ, which provides the real distance between two nodes based on the map (i.e., taking into account the presence of buildings, street curves, and so on), is less than $Th(\Delta)$, that is, the maximum acceptable distance between each node based on the mobile terminal velocity. Weights are then put in a linear relation with distances between nodes, modeling reachability between nodes, and enforcing all known map and motion constraints.

The TFG is then constructed using a two-step process. First, a weight function with fixed $\Delta = 1$ is used, considering only edges between consecutive temporal nodes for which $\mu(e, map) \leq Th(1)$, and nodes with at least one valid inbound or outbound edge. Second, we consider edges between non-consecutive temporal nodes. If no reachable node is found at time $t+k$, nodes at time $t+k+1$ are evaluated. If a reachable node is found, a forwarding edge between non-consecutive temporal nodes is added to the TFG. Figure 2 shows an example of the TFG. Edges with solid lines represent motion between consecutive nodes, and edges with dashed lines model motion between non-consecutive nodes. The selected position nodes and path are in red, while the possible position nodes in black. The best candidate position at each time instant is selected applying a shortest path algorithm on TFG satisfying the weight function $\mu(e, map) \leq Th(\Delta)$. A filtering stage may then be applied to the TFG, such as a constrained Kalman filter (CKF) [26], to further refine and increase the quality of the movement trend obtaining a robust error and time-deep prevision tracking.

In summary, although the proposed geolocation algorithm produces in general good results, there still exist areas in which the signal is poor and the geolocation process suffers of a great error. These areas can be identified by using a sensibility map [3] that considers the position of the antennas and the predicted EMF to model the quality of the signal in every part of the area of interest. In the following, we put forward the idea that an integration of a landmark matching infrastructure within our geolocation algorithm can greatly enhance the quality of geolocation in those area with poor signal.

As we will see, the definition of the landmarks and related infrastructure can be tuned on the basis of the sensibility map.

3 Visual feature-based Filtering

In multiple candidates geolocation, the number of selected candidates positively affects the accuracy of the algorithm, while it negatively impacts the complexity of the algorith. This conflicting scenario must be reconciled to provide a high-quality geolocation suitable for real environments. In Section 2, we suggested a reduction of candidates that uses a map-based filtering technique. This solution however does not reduce the complexity in evaluating each of the multiple candidates selected in the first phase. Based on recent studies,[2] more than 60% of mobile devices are equipped with multimedia functionalities, especially with a digital camera; we then put forward the idea of using a matching framework that compares selected landmarks (e.g., historic buildings) with images taken by the mobile device to improve the geolocation algorithm accuracy, while reducing the number of candidates. The number n of possible candidates for each time instant can be reduced by defining landmarks in strategic areas of the target environment and by then matching them with visual information (e.g., color, shape, texture) of the images taken by the mobile device. In the following of this section, we concentrate on describing the framework used to compare landmarks with digital images, and then in Section 4, we present its integration in the context of our geolocation algorithm.

We consider a Content Based Image Retrieval (CBIR) scenario, where the visual information is analyzed and matched at the server according to images showing landmarks in the target environment. In general, the mobile device captures an image of buildings aroud its position and sends it to the CBIR service responsible for the matching between the image and the defined landmarks. To improve the performances of the process, a rough location of the device is used to restrict the number of landmarks to be used for matching (urban areas provide a good GSM/3G coverage that can be exploited for accessing CBIR services). Usually, a cellID geolocation is adopted, where all landmarks in a cell are used for matching. The low accuracy of cellID geolocation result in a huge number of landmarks to be matched, that highly affect the performances in terms of quality and precision. As we will show in the next section, we use our geolocation algorithm to substantially reduce the area to be used in the selection of the landmarks, thus achieving less landmarks and better performances. Other problems of CBIR techniques in a mobile domain concern the *cost* (e.g., roaming fees, high data transfer, etc.) and the *hardware limitations* (e.g., battery lifetime, display size, etc.). In this case, the minimization of the size of data transfers between the mobile device and the CBIR service is important to reduce the cost as well as some hardware problems. Instead of sending the whole image to be matched to the CBIR service, the necessary low level features can be extracted automatically at the mobile device. For ensuring an interoperable access to the extracted information, the MPEG-7 standard [19] for metadata representation can be used.

In this context, the introduced approach for reducing the candidate set relies on the central idea of the MoidEx [10] project. MoidEx provides a location based mobile tourism (mTourism) system, that supports tourists in receiving information about un-

[2] `http://www.multimediaintelligence.com/`

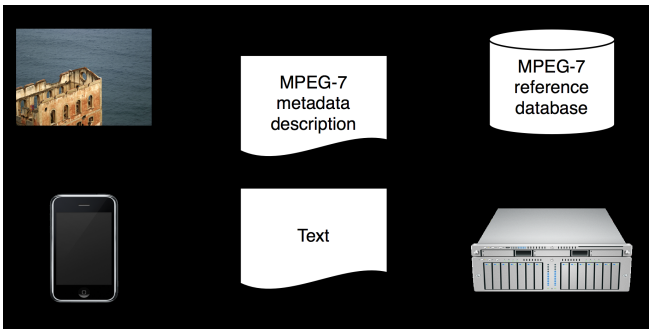

Fig. 3 MoidEx workflow

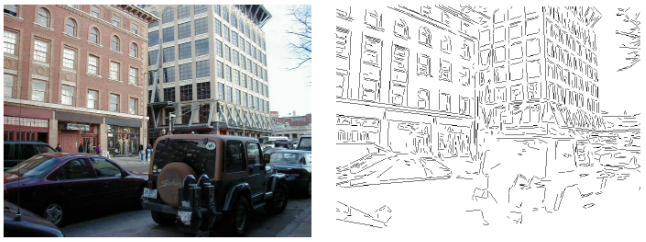

Fig. 4 CLC algorithm: Extraction of straight lines

known objects (e.g., buildings in foreign countries) in a point of interest scenario. For this purpose, a tourist takes an image with a mobile device, as shown in Figure 3. After that, several low-level MPEG-7 features [25] are extracted (e.g., the Scalable Color Descriptor, Edge Histogram Descriptor, Dominant Color Descriptor). Although the Color Layout Descriptor and the Edge Histogram Descriptor both contain information on the spatial distribution of colors and edges, this information is still very coarse and might not be sufficient to reliably recognize the specific structure of a buiding (e.g. a church). Especially in crowded places, occlusion by other objects like cars or buses and different weather conditions might cause additional difficulties. Therefore, to support the identification of buildings in an image, the MoideEx system makes also use of the Consistent Line Cluster (CLC) algorithm [17].

The CLC algorithm is based on the fact that the shape of buildings and other man-made objects typically contains many straight line segments, which come from the boundaries of windows, doors, or the building itself, as shown in Figure 4. Another important observation is that if two line segments belong to different objects, the local colors around them are usually different. In addition, line segments from different objects most likely belong to different spatial groups. Based on these observations, the CLC algorithm uses the color, orientation, and spatial features of line segments to partition them into consistent line clusters, that is, all lines in a cluster have closely related characteristics regarding those features. The relationships of lines in such a cluster and those between different clusters can then be used to allow the recognition of complex objects.

Following the workflow presented in Figure 3, the mobile device creates a valid MPEG-7 instance document which contains all extracted information of the image (low level features and the CLC). Afterwards, this metadata description is sent to the

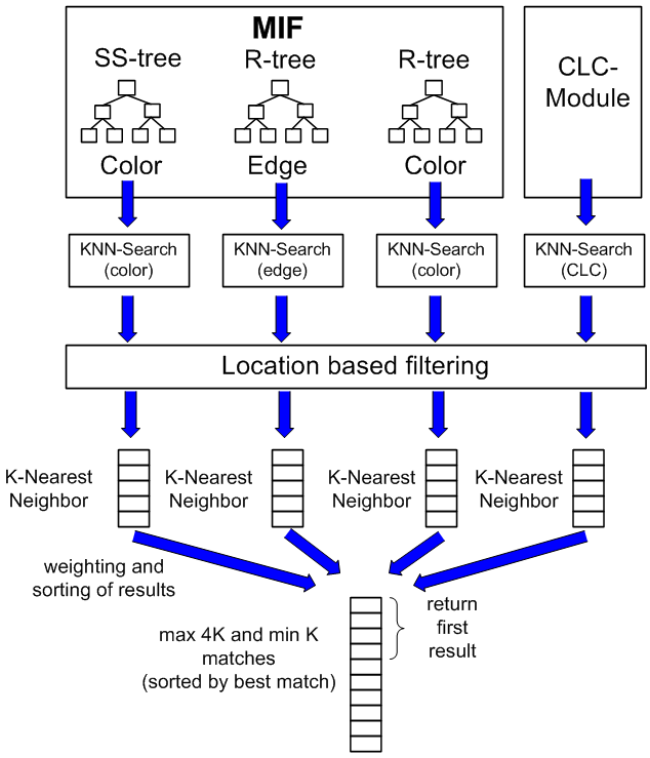

Fig. 5 K-NN retrieval within MPEG-7 MMDB

image retrieval library, which is build on top of the *MPEG-7 Multimedia Database* (MPEG-7 MMDB) [12]. In our scenario, the MPEG-7 MMDB data model features a geolocation database containing images showing landmarks, a description of their exact geographic position and the corresponding low level metadata as MPEG-7 descriptors. In general, the performed similarity search relies on nearest neighbor (NN) retrieval for the extracted features. Relying on the integrated multimedia indexing framework (MIF) several access methods (R-tree, SS-tree) for realizing CBIR functionality are used. In series, the retrieval process proceeds as follows (see Figure 5). Based on the given reference sample description a k-NN-Search is initiated. The k-NN-Search is combined with a location based filtering which restricts the search space to only those buildings that are in the range of the mobile device's location.

The resulting k-NNs are merged together sorted by their occurrences in the respective result sets. For instance, an image has very similar color and edge features in comparison to the reference description then the same image will probably occur in both result sets (color and edge). During the merge process this image will be ranked higher than others that occur only once in the four resulting sets. Then, the candidates in question are thinned out by evaluating whether the position of the resulting nearest neighbor images (only the top most elements are considered) occur in their path. Consequently, paths that cannot be associated with an image position are discarded.

4 Landmark-assisted Geolocation

We present our hybrid geolocation algorithm that integrates landmark definition and matching with DCM. In the following, we first discuss a solution based on a sensibility map to define and select landmarks, and its impact on the geolocation approach. We then describe the hybridization of the landmark solution within our time forwarding algorithm.

4.1 Landmark definition based on a sensibility map

As described in Section 2, our geolocation algorithm based on signal strength and DCM suffers of imprecision due to the inaccuracy of EMF prediction that does not account for fluctuations. To partially counteract this imprecision, we put forward the idea of using a sensibility map to tune the number of candidates based on the signal quality achieved in the area under consideration [3]. The sensibility map we used in [3] exploited map information, antenna positions, number of candidate estimates, to model the error sensitivity of our DCM-based geolocation in simulated environments.

Here, we consider a real environment, which is completely different from a simulated one. As a consequence, we conduct some sensibility oriented campaigns in real environments to evaluate the sensitivity of localization in the areas of interest. More in details, the sensibility of one point (*latitude*, *longitude*) in the area of interest is calculated as follows:

$$Sensibility(lat, long) = argmin_{\forall i, P_{loc,i} \in cand}(dist([lat, long], P_{loc,i})/D_{Max} \qquad (2)$$

where $P_{loc,i}$ gives the i-th location candidate $[lat_x, long_y]$, $cand$ is the set of candidates, $dist([lat, long], P_{loc,i})$ gives the distance between the real position $[lat, long]$ and the i-th candidate, and D_{Max} is the maximum error used as a normalizing factor. In other words the location sensibility on a real position in the map is the normalized smallest distance between this real position and each candidate. The sensibility value is high when the location error is high, while it is low in the case of good location. One simple strategy to improve the precision of location in high sensibility areas is then to increase the number of candidates to achieve a better probability of good estimation after the candidate selection. Although this process may seem reasonable in simulated environments, it is difficult to apply in real scenarios because of the increasing complexity in the candidate selection process.

In this paper, we try to overcome this complexity problem to provide a geolocation algorithm suitable for real environments. To this aim, we introduce a landmark-based geolocation approach, where landmarks are considered as *fiducial points*, meaning that the detection of a landmark is equal to the detection of a high-accurate location. The adoption of landmark matching reduces the complexity of the geolocation process, because there is no need to select an increased number of candidates in areas with high sensibility.

Our solution to the integration of landmark matching still relies on the sensibility map. The sensibility map is constructed a priori and can be used to identify areas where ad-hoc landmarks (*location-oriented landmarks*) can be defined to reduce the location error, still maintaining low complexity. Practically speaking, some landmarks are placed in those areas with high sensibility map, where the probability of poor localization is

high. Of course also the landmark-based location suffers of uncertainty problem but, as we will discuss in the experimental section, it substantially reduces the uncertainty introduced by signal-strength geolocationm especially in high sensibility areas.

Location-oriented landmarks are then landmarks explicitly defined to improve the geolocation algorithm. Traditionally, however, landmarks are used and placed in the maps just for service-oriented purposes. Landmarks in fact are often integrated in LBSs (e.g., [11]) to enhance their functionalities and precision. Our solution can also take advantages from service-oriented landmarks with the only difference that their trustworthiness is considered equal to the trustworthiness of the multiple candidates identified by the geolocation algorithm. As a consequence, the position returned by evaluating service-oriented landmarks cannot be considered as a fiducial point, but rather it becomes an additional candidate to be considered in our algorithm and added to our TFG.

In summary, the set of landmarks in the area of interest can include both location-oriented and service-oriented landmarks. The service-oriented landmark are in general related to a particular point of interest for being useful at the service level (e.g. turism [11]), while location-oriented landmarks are used for localization. Our system uses both of them to improve the precision of location as presented in the following of this section.

4.2 Integrating landmarks with DCM

A location algorithm based on landmarks, as described in Section 3, produces a single location information. The same happens with the DCM approach, in Section 2, that produces one location estimation from a set of multiple candidates based on a time forwarding algorithm. Our enhanced geolocation algorithm aims at combining the two solutions. Two possible approaches have been explored. The first searches for a landmark-based candidate at each time instant t: if available, it is considered as a fiducial point, and used in place of the location obtained via DCM with multiple candidates at time t; otherwise the position retrieved by DCM with multiple candidates is used. This approach consists of a simple composition and makes the two algorithms completely independent. A second approach, used in this paper, consists of a full hybridization of the two solutions. Full hybridization means that landmark infrastructure is integrated inside our time forwarding algorithm in such a way that the entire time forwarding approach takes advantages from the presence of location information of different natures. The main idea of our hybrid approach is to extend the Time Forwarding Graph (TFG) to include the location information produced by the landmark algorithm, while considering the difference between location-oriented and service-oriented landmarks.

As already discussed the TFG is a direct acyclic graph, where every node p_i represents one of the possible positions i of the mobile terminal identified by means of a lookup table, while edges represent motion between pairs of nodes. Each edge is associated with a weight, and computed based on destination reachability and map constraints. After identifying the candidate nodes, the TFG is constructed using a two-step algorithm. In the first step, edges between consecutive temporal nodes (i.e., $\Delta = 1$) are selected based on their reachability, modeled by the weight function in Equation (4). Then, edges between non-consecutive temporal nodes are considered. Let S_{t+k} be the set of candidate positions at time $t + k$. Recalling that, the distance from a node $p_{i,t}$ to a node $p_{j,t+k}$ is the same as the weight W among them, a distance

M can also be defined between a node $p_{i,t}$ and a set of candidate positions S_{t+k} at time $t+k$, according to the map, as follows:

$$M(p_{i,t}, S_{t+k}, map) = min_{j\in[1\cdots n]}(\mu(p_{i,t}, p_{j,t+k}, map)) \quad (3)$$

For each node $p_{i,t}$ of the TFG, if no reachable node is found at time $t+k$, that is, $M(p_{i,t}, S_{t+k}, map) = +\infty$, nodes at time $t+k+1$, with $(k+1) \leq m$, are evaluated. If $M(p_{i,t}, S_{t+k+1}, map) \neq +\infty$, an edge between non-consecutive temporal nodes is added to the TFG.

Here, the TFG is extended to consider also nodes coming from the landmark location. An approach different from the one discussed in Section 3, where the location information on the serving cell id is used to identify the set of available landmarks, is taken to improve performances. In particular, we use the set of n candidates calculated based on DCM, as the means to identify the set of landmarks L to be compared with the image acquired by the mobile device. A solution that uses DCM-based multiple location candidates for identifying landmarks is more accurate and less complex than a solution using the rough serving cell id. Traditionally, urban cells have a minimum radius of ≈300 meters (in our experimental environment in the city of Milan the average cell radius is 500 meters), and, therefore, the location information about the serving cell can be assimilated to the knowledge of a circular area around the serving cell of $\approx 290000m^2$. This area is taken as a reference to identify the available landmarks to be used for matching, that is, all the landmarks included in the circular area. In our approach, instead, we consider a set of 20 candidates with an average error r of $50m$ each (see experiments in [1]), and then we produce n circular areas of radius $50m$ with each candidate used as the center of the circle.[3] The total area generated in the worst case (i.e., no overlapping between the n circles) is of $\approx 160000m^2$ with a reduction of the searching areas of ≈ 45%. This reduction implies a benefit in terms of computational performances (less landmark candidates after location filtering) and quality of landmark matching due to the reduced number of wrong candidates (see Section 5 for more details). Figure 6 shows a graphical comparison of the two approaches to landmark selection. Circles with single lines represent all the areas identified by the set of candidates and used for landmark matching; the big circle with dashed line represents the area of the cell that is traditionally used for the matching. It is clear that, the number of candidates used for matching is likely to be smaller in the first approach, or at least equal in the worst case.

Let us then define $I(S_t, r) \rightarrow l$, with $l \subseteq L$, as the function that takes in input a set S_t of n location candidates and an average error r, and produces in output a set of filtered landmark candidates l, that is, those landmarks included in at least one of the circular areas identified by S_t and r. By further applying a landmark matching function N over the landmark candidates l (i.e., $N(l)$), we potentially obtain a match with either a location-based or a service based landmark, and identify a position $pLand$ to be added to our TFG. More in details, the TFG may include three different types of nodes that are treated differently: *i)* DCM candidates $\{p_1, \ldots, p_n\}$; *ii)* location-oriented landmarks $pLand_{loc}$, and *iii)* service-oriented landmarks $pLand_{serv}$. We can then redefine S_t for each time instant t as following.

[3] We represent each location as planar circular area since it approximates well the actual shape resulting from many location techniques.

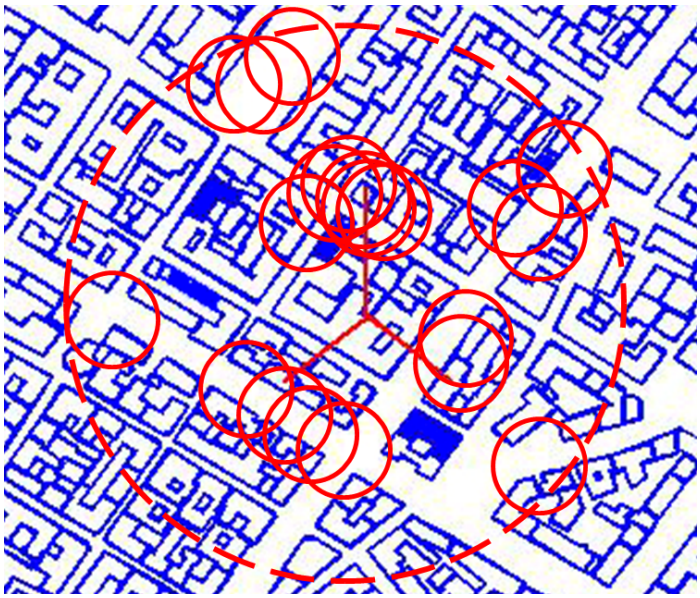

Fig. 6 Landmark Selection

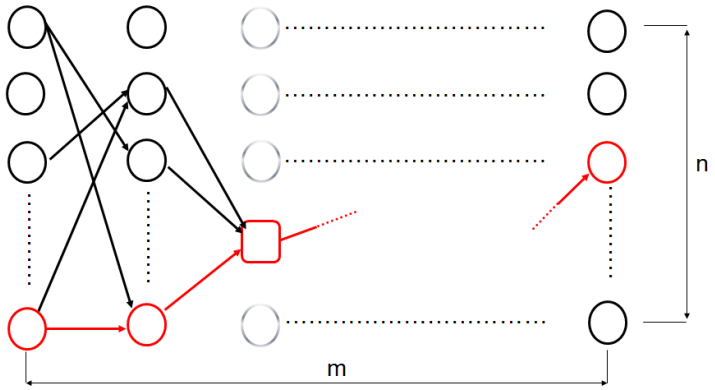

Fig. 7 An example of TFG with the integration of a location-oriented landmark.

$$S_t = \begin{cases} \{p_1, \ldots, p_n, pLand\} & if\ pLand \in pLand_{serv} \\ \{pLand\} & if\ pLand \in pLand_{loc} \\ \{p_1, \ldots, p_n\} & if\ pLand\ is\ not\ detect \end{cases} \tag{4}$$

As presented in System of Equations (4), when a match on a service-oriented landmark is found, S_t has cardinality $n+1$ and contains all DCM-based candidates $\{p_1, \ldots, p_n\}$ plus the identified landmark $pLand \in pLand_{serv}$; when a match on a location-oriented landmark is found and a fiducial point is retrieved, S_t has cardinality 1 and contains $pLand \in pLand_{loc}$ only; when a match is not found, S_t has cardinality n and contains $\{p_1, \ldots, p_n\}$. Each S_t in the forwarding window of the TFG may then

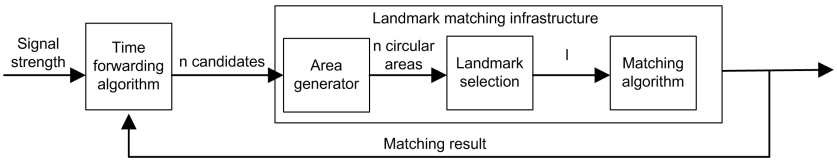

Fig. 8 Landmark-assisted geolocation architecture

contain a variable number of candidates with no fixed cardinality. Figure 7 shows an example of TFG when a location-oriented landmarks is found. The location-oriented landmark at time t is depicted with a red square.

The integration of landmark-based nodes produces also a redefinition of forwarding edges, as follows.

– a forwarding edge e between two non-consecutive temporal nodes $p_{i,t}$ and $p_{j,t+k}$ is included in the TFG, iff $\forall i \in [1,\ldots,k-1]\ \sum_i |S_{t+i}| \geq (k-1)n$:
  1. $min_{h=1\cdots k-1}(M(p_{i,t}, S_{t+h}, map)) = +\infty$ and
  2. $M(p_{i,t}, S_{t+k}, map) \neq +\infty$.

By definition, forwarding edges are forbidden in the TFG if they introduce a jump that skips a location-oriented landmark. On the other hand, a forwarding edge that terminates in S_t={pLand}, with pLand∈pLand$_{loc}$, is permitted. The location-oriented landmark node becomes a "mandatory crossing" node, because it is considered as a trusted point. In the case of service-oriented landmark at time t, the TFG proceeds as usual. Service-oriented landmark nodes are then equivalent to TFG nodes, and can be chosen or not depending on the different paths evaluated by the TFG.

To conclude, Figure 8 shows the architecture of our *landmark-assisted geolocation* algorithm. First, the *time forwarding geolocation* algorithm collects measurements on signal strength and EMF prediction to fill in the lookup table. Then, after receiving the measurements performed by the terminal itself, it produces n position candidates for each time instant t. These candidates are sent to the *landmark matching infrastructure* that: *i)* generates n circular areas around them with radius r, *ii)* selects the set of landmarks l contained in those areas, and *iii)* uses the matching algorithm to compare selected landmarks with the image captured by the camera on the user's device. The result of the matching is returned to the time forwarding geolocation algorithm and can be either the position of a location-based landmark, the position of a service-based landmark, or null. The result is integrated in the TFG and the process repeated for $m-1$ time instants, thus identifying the location and movement of the mobile user.

5 Experimental Results

We set up an experimental environment in the city of Milan, the second largest metropolitan area in Italy with a complex urban environment including parks and skyscrapers. We first performed five trips by car over a month of experimentation with a duration varying from 5 to 20 minutes. Information related to serving and neighboring cells coupled with GPS latitude and longitude have been collected using cellular phones every 0.48 seconds. We then defined 30 location-oriented landmarks in a target area of $2,5km$ x $3km$, based on the sensibility map.

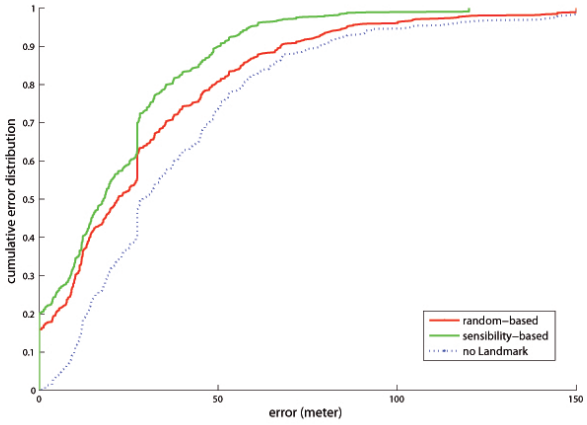

Fig. 9 Cumulative error distribution for experiment (a). A comparison between cumulative error without landmark and with landmark (ad hoc or random chosen)is presented.

Table 1 Comparison of location results (errors-mean square root (in meters)) using: *i)* Signal strength geolocation algorithm in Section 2, *ii)* Hybrid Landmark-assisted geolocation.

		Signal strength-based Approach		**Landmark assisted Approach**		
Exp.	**Dur.**	**mean**	σ	**mean**	σ	**Landmarks**
a	500s	39.39	32.78	23.92	22.49	15/15
b	300s	73	57.93	34.60	40.90	16/16
c	800s	63.62	52.96	25.37	34.66	25/25
d	600s	55.18	48.13	28.35	36.78	15/16
e	300s	45.5	33.67	24.56	30.45	11/11
Mean		55.34	45.09	27.36	33.05	

We extensively test the performance of our landmark-assisted geolocation, in the above environment, by: *i)* analyzing the overall geolocation quality, and then comparing the landmark-assisted geolocation in this paper with the geolocation in Section 2 with no landmark definition; *ii)* providing a comparison between the performance of our algorithm when landmarks are defined in an ad-hoc way using the sensibility map and when they are selected randomly; *iii)* providing, for every test, the rate of landmarks included in our candidate-based searching areas over the total number of landmarks in the serving cell areas, together with the rate of correct landmarks in our searching area.

Figure 9 shows the cumulative error distribution for the first of our five experiments (i.e., experiment (a)). It also shows the comparisons between the geolocation algorithm in Section 2 with no landmark definition, the landmark-assisted geolocation with location-oriented landmarks chosen randomly, and the landmark-assisted geolocation with location-oriented landmarks chosen based on a sensibility map. The performance of geolocation with landmarks selected using the sensibility map overcomes the algorithm using random landmarks; this is expected since, in the first case, landmarks are defined focusing on those areas where geolocation has low precision.

Table 1 presents the results in terms of mean error and variance for the five trips using only location-oriented landmarks. The first experiment (for path (a)) is characterized by a good location estimation even without landmark definition. This is due to the fact that the path resides for ≈ 65% on a low sensibility area with good geolocation quality. Adding few ad-hoc landmarks (e.g., 15), the final precision is really impressive reaching an average error of 23.92 meters with an improvement of ≈ 40%. This result supports our intuition that landmark integration is useful also in environments with low sensibility. Much in line with experiment (a), experiments (c) and (e) provide good results. Experiment (b), instead, considers the shortest timeframe (300 seconds) and covers an area with high sensibility (≈ 75% of the path). In this case, with 15 landmarks, we obtain a less accurate result with an average error of 34.60 meters. To improve the final quality of geolocation and achieve an error similar to the one of experiment (a), we added 4 service-oriented landmarks on the path, thus obtaining a mean error of 25.08 meters with standard deviation of 38.33 meters.

Finally, in experiment (d), where 15 landmarks are still defined in the area of interest, one landmark is not detected. This scenario may happen in areas with high sensibility where the precision of our geolocation is poor. In this case, in fact, it is possible that no landmarks are within the areas with radius of 50 meters identified by the selected candidates. This is an effect of our approach to landmark selection in Section **??** that reduces of ≈ 45% the searching area. Although, this solution greatly improves the performance of the landmark matching engine, it relies on the assumption that at least a candidate is near (50 meter) to the landmark position. As an example, whereas with the cellID approach the average number of landmark is 12, with our approach we have an average of 5 landmarks for each path in the searching areas,[4] with a minimum value of 3 landmarks for path (a) and a maximum value of 8 landmarks for path (e). In the same way of experiment (b), it is possible to improve the quality of experiments (d) by adding some service-oriented landmarks. One interesting result, when service-oriented landmarks are added, is that also the landmark not selected in the previous experiment (let call it "unused landmark") is now used. This is the effect of the hybridization of landmark matching and signal-based geolocation in the same algorithm. When a new service-oriented landmark is selected, this choice influences the forwarding path chosen by the forwarding algorithm. If the selected service-oriented landmark is spatially near to the "unused landmark", it is likely that the "unused landmark" is selected and then becomes part of the path.

To conclude, an interesting aspect to discuss is what happen for the same set of experiments when a non-hybrid technique is used. A non-hybrid technique must follow this simple rule: "if a landmark is localized, then use the landmark; otherwise use the signal geolocation", meaning that landmark selection does not influence the geolocation algorithm. The results achieved by our experiments are summarized in Table 2

It is clear that the hybrid approach outperforms the non-hybrid approach in our experimental set, because of the positive influence of landmark-based candidates on the choice of the forwarding path. More in details the mean error in the case of Hybrid approach is reduced by ≈ 35% while the standard deviation is reduced by ≈ 20%.

[4] Note that, this strongly depends on the density of landmark in the area

Table 2 Location error using a non Hybrid approach.

		Non Hybrid approach	
Exp.	**Dur.**	**mean**	σ
a	500s	32.69	29.38
b	300s	52.44	49.82
c	800s	43.32	54.13
d	600s	47.65	42.32
e	300s	33.35	32.67
Mean		41.89	41.66

6 Related work

Geolocation of mobile devices is an important topic in the area of mobile computing, and has been exploited for several different purposes ranging from the support of crucial tasks for network management (e.g., handoff management, efficient code division in 3G networks) to the support for high quality location-based services (LBSs).

A fundamental requirement for every solution providing geolocation and mobility prediction is the provisioning of high reliable and accurate approaches that work well regardless of the considered environment. First location techniques were based on time measurements, such as, *Time of Arrival* (ToA), *Time Difference of Arrival* (TDoA), *Enhanced-Observed Time Difference* (E-OTD) [14, 21]. These techniques suffer in urban environments, where scenarios with no line-of-sight between the mobile terminals and the base stations are common, and the accuracy of the estimated position heavily depends on the number of measurements and on the placement of the antennas supporting triangulation. Subsequent location techniques, based on RSSI which measures signal attenuation, have been provided with the strong assumptions of having free space propagation of the signal and omnidirectional antennas. RSSI-based mobile terminal location can be reduced to the problem of triangulation and is influenced by physical phenomena that affect radio propagation and location precision (e.g., reflection, diffraction). As a consequence, RSSI location estimation does not fit well to urban areas, and results in imprecise geolocation. To improve the geolocation results, several solutions to model and predict electro-magnetic signal propagation have been provided, such as, advanced deterministic models (ray-tracing, IRT [28]), empirical (Hata-Okumura [22], Walfisch-Ikegami [8]), and hybrid techniques (Dominant Path [29]). Although prediction models improve the accuracy of geolocation, many problems still influence the geolocation process. Among them, EMF fluctuation is the most important that has been already considered in past research and also discussed in this paper. An interesting approach to deal with EMF fluctuations used vector regression [30]. Regression techniques model the location problem as a *checkpoint location*, which can be solved as a machine learning problem. However, real data sampling are not always available and the need for a training phase affects the applicability of many machine learning techniques in practical scenarios. Some techniques exploited databases containing RSSI predictions or measurements (i.e., database correlation). Database correlation is affected by an intrinsic measurement error of RSSI that many recent works try to overcome applying *filtering* techniques with mobile motion model. Anisetti et al. [1] used a lookup table for multiple candidate selection (much in line with RADAR system developed by Microsoft research [4] for wireless networks) and identified the number of candidates based on geographical region and GIS information. In addition, to improve

the quality of geolocation and tracking, a filtering stage on the identified movement trend is applied using a Constrained Kalman Filter (CKF) [26]. Zaidi and Mark [32] presented two algorithms for real-time tracking, location, and dynamic motion of a mobile station in a cellular network. The proposed solution is based on pre-filtering and two Kalman filters, one to estimate the discrete command process and the other to estimate the mobility state. Yang and Wang [31] proposed a Monte Carlo algorithm for cell hand-off decision based on mobility tracking in cellular networks. The location and speed of a mobile terminal are exploited to predict the signal strength in future time instants, and forecast the hand-off time. Zhang et al. [33] studied the performance of target tracking in the presence of nonlinear road constraints using a constrained Extended Kalman Filter (EKF). Finally, Mihaylova et al. [20] presented a solution based on RSSI and map information that exploits particle filtering and is tested with data coming from a real network.

Recently, some works have focused on exploiting the availability of mobile devices that integrate several different sensors to improve the accuracy of location techniques. Similarly to the work in this paper that integrates a location technique based on DCM and RSSI with images captured by the device camera and landmark matching, other solutions have been provided that integrate GSM/GPS geolocation with data from camera, accelerometers, and the like. For instance, in the 3G version of the iPhone a GPS chipset is used, and WiFi positiong and cell data exploited to make the GPS initialization faster. Also, accelerometers are used for tracking users moving in low speed areas.

Some approaches hybridize different algorithms but using the same type of signals like [5] that uses time delay information for Hybrid AOA/TDOA Geolocation, others uses different type of signals but in some sense coming from the same source (the wireless network), like [24] that uses Signal strength and Time of Arrival. These hybridization uses signals that are in some sense correlated (e.g. a infrastructure problem on network impacts on both). In our case the hybridization is with signal of totally different nature and not correlated. Other approach like [23] uses signal of different nature (Radio Frequency Identification (RFID) and GPS) for positioning of pedestrians in areas where no GNSS position determination is possible due to obstruction of the satellite signals. They proposed a strong hybridization with GNSS using enhanced MRERA. One interesting approach that like us takes advantages of video sensor is [15] that combines a GPS and an inertial sensor with a camera to provide accurate localization, but just for improving Augmented Reality in outdoor environment and not for geolocation purposes.

Focusing on LBS, some applications already supported object recognition and/or location based services. The George Square2 project aimed at enabling collaboration as a port of leisure [6]. The goal is to enable two users sharing their traveling experiences with another. Mobile users carry a tablet PC, which is connected to the Internet and is equipped with a GPS receiver, a camera, and a headset used for voice-over-IP communication. A special software keeps track of the user's location and the user's activities. One way to provide information on points of interest, besides the use of the location, is the support of object recognition with mobile phones. For instance, mobileor5 used cell phones with integrated cameras to identify certain objects. It used the SIFT (Scale-Invariant Feature Transform) algorithm [18], which can be classified as an appearance-based object recognition approach. Another system supporting object recognition is PhoneGuide [7]. It is a museum guidance system running on cellular phones. The goal is to provide museum visitors with additional multimedia information

on the exhibit they are currently watching, without interfering with the exhibition itself. To reliably identify the current exhibit, PhoneGuide employs object recognition as well as location information. A location-based touristic guide called mTourist [11] uses geolocation and landmarks to guide the tourists through a city. The position of the user is calculated through CellID. Based on the cell, a set of landmarks is identified and used to release the touristic service and refine the user position.

7 Conclusions and Future Work

We presented a landmark-assisted geolocation algorithm that integrates and hybridizes a geolocation solution based on RSSI and DCM with a landmark matching framework. The proposed solution builds on the definition of location-oriented landmarks in those areas with high sensibility map, to reduce the complexity introduced by the need of multiple candidates for accurate geolocation. Also, the solution takes advantages by existing service-oriented landmarks used for the provisioning of location-based services. Our experiments show the improvements in terms of quality of geolocation with respect to geolocation that does not exploit landmarks, also in those contexts where landmarks are randomly distributed.

Beside benefits in terms of location accuracy and complexity, our hybrid solution can provide advantages also for those applications that rely on geolocation and landmarks to provide LBSs. Important aspects to consider in the deployment of such applications for cellular networks are the costs needed for the communication, the accuracy, and availability of the positioning process, and the requirements in terms of performances and hardware of the devices. In this context, a common drawback shared by existing techniques is that they usually rely on inaccurate location techniques (e.g., CellID) resulting in solution with low performance, low accuracy, and high overhead. A lightweight and accurate positioning system like the one in this paper can be integrated with applications that are based on landmark matching providing high performance and success rate.

References

1. M. Anisetti, C.A. Ardagna, V. Bellandi, E. Damiani, and S. Reale. Advanced localization of mobile terminal in cellular network. *International Journal of Communications, Network and System Sciences (IJCNS)*, 1:95–103, February 2008.
2. M. Anisetti, C.A. Ardagna, V. Bellandi, E. Damiani, and S. Reale. Method, system, network and computer program product for positioning in a mobile communications network. In *European Patent EP1765031*, Published in date 21 March 2007.
3. M. Anisetti, V. Bellandi, E. Damiani, and S. Reale. Localization and tracking of mobile antenna in urban environment. In *Proc. of the International Symposium on Telecommunications*, Shiraz, Iran, September 2005.
4. P. Bahl and V. N. Padmanabhan. Radar: An in-building RF-based user location and tracking system. In *Proc. of the IEEE INFOCOM 2000*, Tel-Aviv, Israel, March 2000.
5. Ali Broumandan, Tao Lin, John Nielsen, and Gérard Lachapelle. Practical results of hybrid aoa/tdoa geo-location estimation in cdma wireless networks. In *VTC Fall*, pages 1–5, 2008.
6. B. Brown, M. Chalmers, M. Bell, M. Hall, I. MacColl, and P. Rudman. Sharing the square: collaborative leisure in the city streets. In *Proceedings of the ninth conference on European Conference on Computer Supported Cooperative Work (ESCW)*, pages 427–447, New York, NY, USA, 2005. Springer-Verlag.

7. E. Bruns, B. Brombach, T. Zeidler, and O. Bimber. Enabling mobile phones to support large-scale museum guidance. *IEEE MultiMedia*, 14(2):16–25, 2007.
8. E. Damosso. COST 231: Digital mobile radio towards future generation systems. *Final report, European Commission*, Bruxelles, 1999.
9. G. Djuknic and R. Richton. Geolocation and assisted GPS. *IEEE Computer*, February 2001.
10. M. Döller, G. Köckerandl, S. Jans, and L. Limam. MoidEx: Location-based mTourism system on mobile devices. In *Proc. of International Conference on Multimedia Computing and Systems*, 2009.
11. M. Döller, G. Köckerandl, S. Jans, and L. Limam. MoidEx: Location-based mTourism system on mobile devices. In *IEEE International Conference on Multimedia Computing and Systems, ICMCS'2009*, apr. 2009.
12. M. Döller and H. Kosch. The MPEG-7 Multimedia Database System (MPEG-7 MMDB). *Journal of Systems and Software*, 81(9):1559–1580, 2008.
13. W. Figel, N. Shepherd, and W. Trammell. Vehicle location by a signal attenuation method. *IEEE Transaction Vehicular Technology*, VT–18:105–110, November 1969.
14. F. Gustafsson and F. Gunnarsson. Mobile positioning using wireless networks: possibilities and fundamental limitations based on available wireless network measurements. *IEEE Signal Processing Magazine*, 22(4):41–53, 2005.
15. J-Y. Didier M. Mallem I.M. Zendjebil, F. Ababsa. On the Hybrid Aid-Localization for Outdoor Augmented Reality Applications. In *ACM symposium on Virtual reality software and technology*, 2008.
16. H. Laitinen, J. Lahteenmaki, and T. Nordstrom. Database correlation method for GSM location. *Proceedings of the IEEE VTC conference*, 2001.
17. Y. Li and L.G. Shapiro. Consistent line clusters for building recognition in CBIR. In *Proceedings of the 16th International Conference on Pattern Recognition (ICPR)*, pages 952–956, Washington, DC, USA, 2002. IEEE Computer Society.
18. D.G. Lowe. Object recognition from local scale-invariant features. In *Proceedings of the International Conference on Computer Vision*, pages 1150–1157, Washington, DC, USA, 1999. IEEE Computer Society.
19. J.M. Martinez, R. Koenen, and F. Pereira. MPEG-7. *IEEE Multimedia*, 9(2):78–87, April-June 2002.
20. L. Mihaylova, D. Angelova, S. Honary, D. R. Bull, C.N. Canagarajah, and B. Ristic. Mobility tracking in cellular networks using particle filtering. *IEEE Transaction on Wireless Communications*, 6(10):3589–3599, October 2007.
21. D. Munoz, F.B. Lara, C. Vargas, and R. Enriquez-Caldera. *Position Location Techniques and Applications*. Academic Press, 2009.
22. Y. Okumura, E. Ohmori, T. Kawano, and K. Fukuda. Okumura-hata propagation prediction model for UHF range, in the prediction methods for the terrestrial land mobile service in the VHF and UHF bands. *ITU-R recommendation P.529-2, Geneva: ITU*, 1995.
23. Guenther Retscher and Qing Fu. Integration of rfid, gnss and dr for ubiquitous positioning in pedestrian navigationn. *Journal of Global Positioning Systems*, 6:56–64, 2007.
24. Bamrung Tau Sieskul, Feng Zheng, and Thomas Kaiser. A hybrid ss-toa wireless nlos geolocation based on path attenuation: mobile position estimation. In *WCNC'09: Proceedings of the 2009 IEEE conference on Wireless Communications & Networking Conference*, pages 2744–2749, Piscataway, NJ, USA, 2009. IEEE Press.
25. T. Sikora. The MPEG-7 Visual Standard for Content Description An Overview. *IEEE TRANSACTIONS ON CIRCUITS AND SYSTEMS FOR VIDEO TECHNOLOGY*, 11(6):696–702, 2001.
26. D. Simon and T. Chia. Kalman filtering with state equality constraints. *IEEE Transactions on Aerospace and Electronic Systems*, 39, January 2002.
27. H.L. Song. Automatic vehicle location in cellular communications systems. *IEEE Transaction Vehicular Technology*, 43:902–908, November 1994.
28. G. Wölfle, R. Hoppe, and F.M. Landstorfer. A fast and enhanced ray optical propagation model for indoor and urban scenarios, based on an intelligent preprocessing of the database. In *Proc. of IEEE PIMRC*, Osaka, Japan, September 1999.
29. G. Wölfle, R. Wahl, P. Wildbolz, and P. Wertz. Dominant path prediction model for indoor and urban scenarios. In *Proc. of the 11th COST 273 MCM*, Duisburg, Germany, September 2004.
30. Z.-L. Wu, C.-H. Li, J.K.-Y. Ng, and K.R.P.H. Leung. Location estimation via support vector regression. *IEEE Transactions on Mobile Computing*, 6, March 2007.

31. Z. Yang and X. Wang. Joint mobility tracking and hard handoff in cellular networks via sequential monte carlo filtering. In *Proc. of the IEEE Infocom 2002*, New York, USA, June 2002.
32. Z. R. Zaidi and B. L. Mark. Real-time mobility tracking algorithms for cellular networks based on kalman filtering. *IEEE Transaction on Mobile Computing*, 4(2):195–208, March/April 2005.
33. M. Zhang, S. Knedlik, and O. Loffeld. On nonlinear road-constrained target tracking in gsm networks. In *Proc. of the IEEE Vehicular Technology Conference (VTC)*, Marina Bay, Singapore, May 2008.
34. D. Zimmermann, J. Baumann, M. Layh, F. Landstorfer, R. Hoppe, and G. Wölfle. Database correlation for positioning of mobile terminals in cellular networks using wave propagation models. In *Proc. of the 60th IEEE Vehicular technology conference (VTC)*, Los Angeles, USA, September 2004.